

Fluctuation theorem and natural time analysis

N. V. Sarlis,¹ P. A. Varotsos,^{1,*} and E. S. Skordas¹

¹*Solid State Section and Solid Earth Physics Institute, Physics Department,
University of Athens, Panepistimiopolis, Zografos 157 84, Athens, Greece*

Upon employing a natural time window of fixed length sliding through a time series, an explicit interrelation between the variability β of the variance $\kappa_1 (= \langle \chi^2 \rangle - \langle \chi \rangle^2)$ of natural time χ and events' correlations is obtained. In addition, we investigate the application of the fluctuation theorem, which is a general result for systems far from equilibrium, to the variability β . We consider for example, major earthquakes that are nonequilibrium critical phenomena. We find that four (out of five) mainshocks in California during 1979-2003 were preceded by β minima lower than the relative thresholds deduced from the fluctuation theorem, thus signalling an impending major event.

PACS numbers: 05.70.Ln, 05.40.-a, 89.75.Da, 91.30.Ab

Entropy production is a measure of the irreversibility of a thermodynamic process: the difficulty, even impossibility, of reversing the observed often macroscopic behavior of a system that exchanges heat or matter with a complex environment (e.g., see Ref.[1] and references therein). The breakage of time reversal symmetry associated with thermodynamic irreversibility has focused enormous discussion for more than a century. Despite of such concerns, however, the concept of entropy generation in the thermodynamics of large systems has been applied widely. From microscopic point of view, efforts towards understanding the nature of the entropy and its production -mainly focused on the one way character of the second law- have been attempted. They modelled the microscopic evolution of a system and its environment in the frame of stochastic dynamics [2] and stochastic thermodynamics [3–5], but interpretations based on deterministic dynamics (e.g., see Ref.[6]) were also forwarded.

An intense interest towards the latter interpretations has been renewed when Evans, Cohen and Morris in 1993 considered the fluctuations of the entropy production rate in a shearing fluid, and proposed the so-called fluctuation relation or the first fluctuation theorem [7]. This is considered [8] to represent a general result concerning systems arbitrarily far from equilibrium. The proof of the fluctuation [9] and related theorems [10] shows how irreversible macroscopic behavior arises from time reversible microscopic equations of motion. The two theoretical results that illustrate this clearly are the second law inequality [11] and the very recent mechanical proof [12] of Clausius' inequality without the prior assumption of the second "law" of thermodynamics. These two results have been obtained without treating the nonequilibrium entropy, but used instead a quantity termed dissipation function first defined [13] in 2000. On the basis of this function, being a path function and not a state function, the relaxation of a system to equilibrium, which is inherently a nonequilibrium process, can be quantified [14].

It has been emphasized in Ref. [6] that, unlike linear

irreversible thermodynamics, the fluctuation and related theorems are exact for systems of arbitrary size as well as for systems arbitrarily near to, or far from equilibrium, as mentioned. This is why we shall employ here the fluctuation theorem for the purpose of the present study.

This theorem [7, 9, 15–19] gives a general formula for the probability ratio that in a thermostated dissipative system, the time average entropy production $\bar{\Sigma}_t$ takes a value A to minus the value $-A$,

$$Pr(\bar{\Sigma}_t/k_B = A)/Pr(\bar{\Sigma}_t/k_B = -A) = \exp[At] \quad (1)$$

from which it is obvious that as the averaging time or system size increases, it becomes exponentially likely that the entropy production will be positive. The theorem was initially proposed [7] for nonequilibrium steady states that are thermostated in such a way that the total energy of the system is constant. Subsequently, it was shown [18, 19] that this theorem can be proved for sufficiently chaotic, iso-energetic nonequilibrium systems using the Sinai-Ruelle-Bowen measure, as well as for purely Hamiltonian systems with or without applied dissipative fields [20] and for a wide class of stochastic nonequilibrium systems [21, 22].

It is one of the two basic aims of this paper to investigate for the first time the application of the fluctuation theorem to the case of earthquakes which may be considered (e.g. [23, 24]) as nonequilibrium critical phenomena (the mainshock being the new phase). They exhibit complex correlations in time, space and magnitude M which have been recently studied by several workers (e.g., see Refs. [25–29]). In particular, the present investigation will be made by applying the fluctuation theorem to the order parameter fluctuations that result from the analysis of the time series in a new time domain termed [30] natural time χ . This is so, because natural time analysis allows us to identify [31] when a complex system approaches a critical point (for a review see Ref. [32]) and in addition enables the introduction of an order parameter for seismicity. The present study has been motivated by the following two findings related to the variability β (defined below) of the order parameter of seismicity [33]:

*Electronic address: pvaro@otenet.gr

First, it captures the events' correlations, as shown here (see Appendix), which constitutes the other basic aim of this paper. Second, the quantity β exhibits characteristic minima [34] before the occurrence of major events.

In a time series comprising N earthquakes, the natural time $\chi_k = k/N$ serves as an index for the occurrence of the k -th earthquake. In natural time analysis the pair (χ_k, Q_k) is studied, where Q_k is the energy released during the k -th earthquake of magnitude M_k . One may alternatively study the pair (χ_k, p_k) , where $p_k = Q_k / \sum_{n=1}^N Q_n$ is the normalized energy released during the k -th earthquake, and Q_k -and hence p_k - is estimated through the relation [35] $Q_k \propto 10^{1.5M_k}$. The variance $\kappa_1 (= \langle \chi^2 \rangle - \langle \chi \rangle^2)$ of χ weighted for p_k , is given by [30, 33, 36, 37]

$$\kappa_1 = \sum_{k=1}^N p_k (\chi_k)^2 - \left(\sum_{k=1}^N p_k \chi_k \right)^2 \quad (2)$$

This quantity, as shown in Ref. [33], can be also considered as an order parameter for seismicity.

The fluctuations of κ_1 , are studied by applying the following procedure [32]. Taking an excerpt of a seismic catalog comprising $W (\geq 100)$ successive events, we start

from the first EQ and calculate the first 35 κ_1 values for 6 to 40 consecutive EQs. Then we proceed to the second EQ, and calculate again 35 values of κ_1 from the 7-th to the 41-st event. Thus, scanning event by event the whole excerpt of W earthquakes, we calculate the average value $\mu(\kappa_1)$ and the standard deviation $\sigma(\kappa_1)$ of the κ_1 values. The quantity

$$\beta \equiv \sigma(\kappa_1) / \mu(\kappa_1) \quad (3)$$

is defined[38] as the variability β of κ_1 for this excerpt of length W . In some occasions, as in the present case, it is of prominent importance to know what happens to the β value until just before the occurrence of each EQ, e_i , in the seismic catalog. We then calculate first the κ_1 values using the *previous* $l=6$ to 40 consecutive EQs. These 35 κ_1 values are associated with the EQ e_i , but we clarify that EQ e_i has not been employed for their calculation. The β value -corresponding to the EQ e_i - for a natural time window length W is computed using all the $(35 \times W)$ κ_1 values associated with the EQs e_{i-W+1} to e_i . The resulting value is denoted by β_W , where the subscript W shows the natural time window length, and the corresponding minimum is designated by $\beta_{W,min}$.

It is shown that the quantity β when using l consecutive events is interrelated with the event's correlations through

$$\beta = \frac{\sqrt{-\sum_{\text{all pairs}} \left[\left(\frac{m}{l} - \langle \chi \rangle_{\mathcal{M}} \right)^2 - \left(\frac{j}{l} - \langle \chi \rangle_{\mathcal{M}} \right)^2 \right]^2 \text{Cov}(p_j, p_m) - \left[\sum_{\text{all pairs}} \frac{(j-m)^2}{l^2} \text{Cov}(p_j, p_m) \right]^2}}{\kappa_{1,\mathcal{M}} + \sum_{\text{all pairs}} \frac{(j-m)^2}{l^2} \text{Cov}(p_j, p_m)}, \quad (4)$$

where $\langle \chi \rangle_{\mathcal{M}}$ and $\kappa_{1,\mathcal{M}}$ correspond to the average value of χ and κ_1 , respectively, obtained when substituting for p_k the average -within an excerpt of W events- values μ_k of p_k ; the symbol $\text{Cov}(p_j, p_m)$ stands for covariance, i.e., the average value of $(p_j - \mu_j)(p_m - \mu_m)$ within the excerpt of W events. The details of the derivation of Eq.(4) are given in the Appendix.

The selection of the W value used for the purpose of our study is of crucial importance. It is taken equal to the number of the events that would occur in a few months, or so, in view of the following: Low frequency (≤ 1 Hz) electric signals, termed Seismic Electric Signals (SES), appear before earthquakes [39, 40]. They are emitted from the future focal region [41] (see also Ref. [42]) when in the focal region the stress reaches a *critical* value σ_{cr} , and then a *cooperative* orientation of the electric dipoles occurs. This leads to the emission of a transient electric signal that constitutes an SES. Several such signals within a short time are termed SES activity [36, 37, 42, 43]. For example, the three lower channels in Fig.1(b) show three SES activities that preceded major earthquakes in western, southwestern and southern Greece, respectively, as depicted in the map of Fig.1(a). (Only for earthquakes of magnitude 6.0 or larger the SES activities are publicized, see p.102 of Ref.[44].) Furthermore, for the sake of comparison, the upper channel in

Fig.1(b) shows a recent SES activity initiated on 8 January 2013 at a station labelled LAM in Fig. 1(a) in central Greece (cf. On 4 June 2013 an $M_L 4.3$ earthquake occurred at $37.98^\circ\text{N}24.01^\circ\text{E}$, i.e., around 20km E of Athens (ATH), which is consistent with the earlier finding[44] in 1999 that LAM station is sensitive to seismic areas close to ATH. The analysis, which was made by following Ref.[45], continued after this earthquake and showed the following results: The probability $\text{Prob}(\kappa_1)$ of the κ_1 values of seismicity in the area $N_{37.7}^{39.0} E_{22.6}^{24.2}$ maximized at $\kappa_1 = 0.070$ on 11 & 12 June 2013 exhibiting magnitude threshold invariance for magnitudes in the range $M_{thres} = 2.2$ to 2.6, see Fig.2, although the completeness of the seismic catalog for such small magnitude thresholds is unclear. These results seem to suggest that the system approaches the critical point and conforms with the fact that a sequence of additional SES activities were recorded at LAM from 31 March to 11 April 2013, see also Refs.[46–51]). The following important fact has just

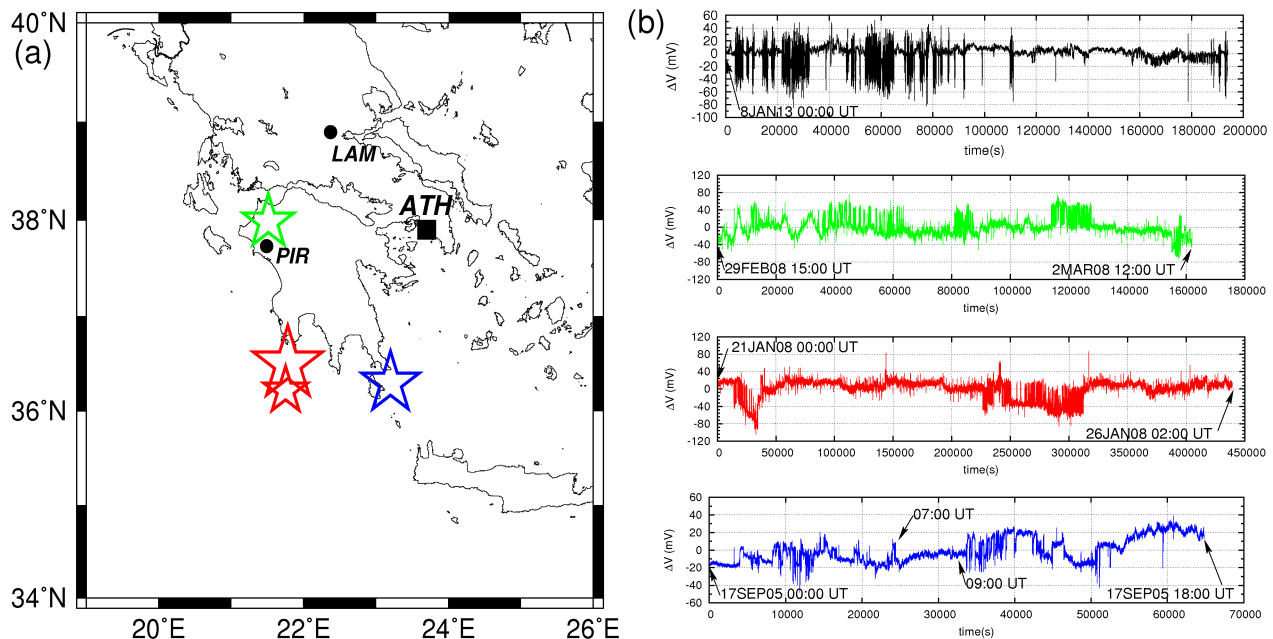


FIG. 1: (color online) (a) Major earthquakes in Greece on 8 June 2008 (green, magnitude $M_w = 6.4$), 14 February 2008 (red, $M_w = 6.9$ and 6.4) and 8 January 2006 (blue, $M_w = 6.7$). (b) Their preceding SES activities recorded at Pargos (PIR) measuring station located in western Greece are shown (with the corresponding color) in the lower three channels. Furthermore, an SES activity initiated recently on 8 January 2013 at a station in central Greece labelled LAM in (a) is depicted in the upper channel of (b). Additional SES activities were recorded at LAM from 31 March to 11 April 2013, see also Ref.[46]

been identified [52]: At the initiation of an SES activity, which usually occurs a few months (with an upper limit of around 5 months) before a major EQ, a clearly detectable change in seismicity appears, manifested by a minimum $\beta_{W,min}$ in the fluctuations of the order parameter of seismicity. Hence, in the case that geolectrical data are lacking, once we identify the date of $\beta_{W,min}$ (by analyzing solely seismic data) this reveals also the date of an SES activity that would have been recorded.

Along these lines, Table I shows the dates of the minima $\beta_{W,min}$ of seismicity before major mainshocks in California during the 25 year period 1 January 1979 to 1 January 2004. We used the United States Geological Survey Northern California Seismic Network catalog available from the Northern California Earthquake Data Center, at the http address: www.ncedc.org/ncedc/catalog-search.html, hereafter called NCEDC. The seismic moment M_0 , which is proportional to the energy release during an earthquake and hence to the quantity Q_k used in natural time analysis, is calculated [32] from the relation $\log_{10}(M_0) = 1.5M + \text{const}$, where the earthquake magnitudes reported in this catalog are labelled with M . The earthquakes with $M \geq 2.5$ reported by NCEDC, within the area $N_{31.7}^{45.7} W_{127.5}^{112.1}$ have been considered. We have on average $\sim 10^2$ EQs per month since 31832 earthquakes occurred for the 25 year period from 1 January 1979 to 1 January 2004. Thus, we adopted natural time window lengths $W=200$ and $W=300$.

The results of this analysis are depicted in Fig. 3(a),(b)

where we plot the variability β (in red for $W=200$ and in blue for $W=300$) versus the conventional time for the periods (a) 1 January 1979 to 1 January 1990 and (b) 1 January 1990 to 1 January 2004. An inspection of these results lead to the $\beta_{W,min}$ values inserted in Table I: In five out of the six mainshocks we find values of $\beta_{300,min}$ and $\beta_{200,min}$ that appear 1 to 5 months before mainshocks. In these five cases $\beta_{200,min}$ varies between 0.324 to 0.474 and $\beta_{300,min}$ between 0.378 and 0.472. We note that the key criterion to distinguish the true precursory $\beta_{W,min}$ from the non precursory ones is the following [34]: The minimum should be followed (before the occurrence of the mainshock) by a period during which the exponent α of the Detrended Fluctuation Analysis (DFA) [54] -calculated for a length $W=300$ events in the magnitude time series- reaches a minimum α_{min} slightly smaller than 0.5 (thus, indicating anticorrelated behavior, but close to random) and then $\beta_{200} > \beta_{300}$. This inequality means that when the system approaches closer to the critical point -which is the case when considering $W=200$ events compared to $W=300$ events- the fluctuations of the order parameter become more intense.

We now proceed to the investigation of Eq.(1) in the case of seismicity and analyze the statistical distribution of the experimentally determined β_W for $W=200$ or 300 , which is clearly path depended. The quantity β_W can be considered as an entropic measure (see Appendix), but its sign is by definition always positive. Thus, in order to apply Eq.(1), we need to define a threshold value $\beta_{W,0}$ above which the entropy production may be considered

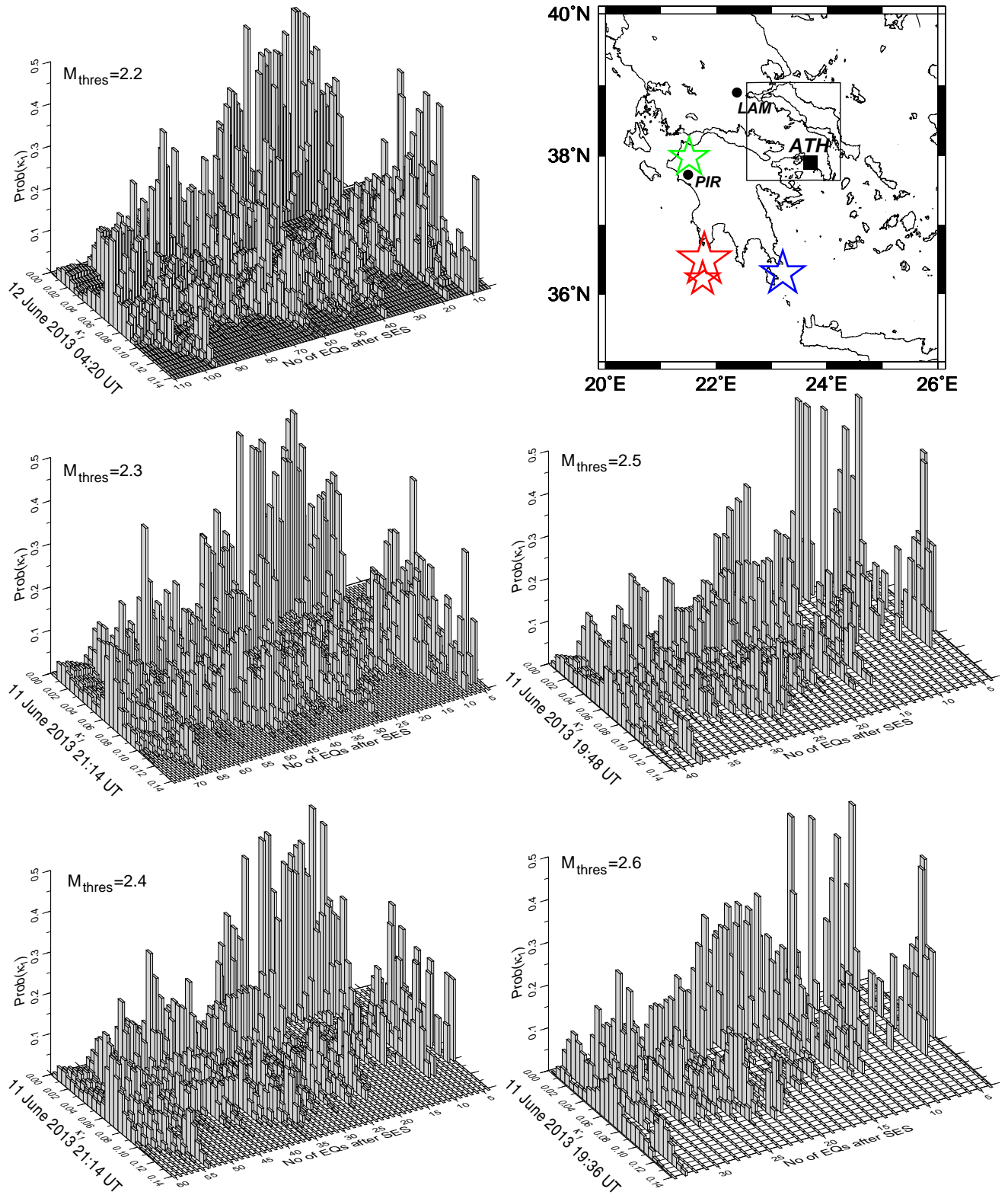


FIG. 2: (color online) The probability $\text{Prob}(\kappa_1)$ as it results from the analysis of seismicity after the initiation of the SES activity depicted in the upper panel of Fig.1(b) within the rectangular area depicted in the map (uppermost right) for various magnitude thresholds M_{thres} . The date and time of the most recent earthquake considered into the calculation (upon the occurrence of which $\text{Prob}(\kappa_1)$ maximized at $\kappa_1 = 0.070$) is written in each case.

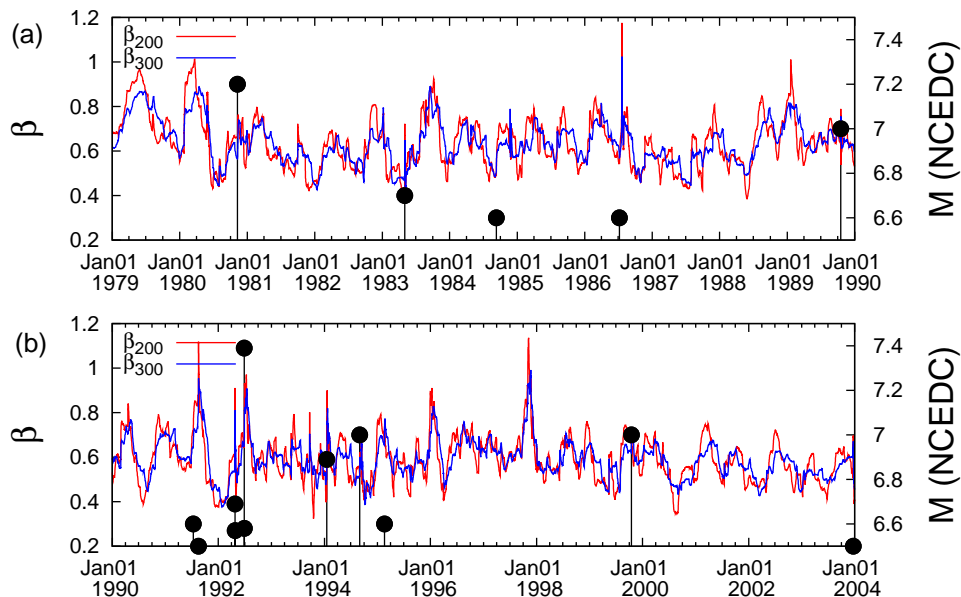


FIG. 3: (color online) The variability β of κ_1 (left scale) plotted versus the conventional time for a natural time window of length $W = 200$ events (red) and $W = 300$ events (blue) during the period: (a) 1 January 1979 to 1 January 1990 and (b) 1 January 1990 to 1 January 2004. The earthquakes with $M \geq 6.5$ (right scale) are shown with vertical bars ending at solid circles.

TABLE I: The minimum DFA exponent α_{min} along with the values of the minima observed for the variability β together with the dates of their observation in parentheses before all major EQs in California with $M \geq 7.0$ within $N_{31.7}^{45.7} W_{127.5}^{112.1}$ during the period 1979-2003. The $M6.9$ Northridge earthquake is also added in italics. The lead time Δt for each case, estimated from the difference in the dates between the EQ occurrence and the appearance of $\beta_{300,min}$ is shown in the last column. The values for $\beta_{300,min}$ and α_{min} are taken from Ref. [34]

EQ Date	EQ Name epicenter	M	$\beta_{300,min}$ (date)	$\beta_{200,min}$ (date)	α_{min} (date)	Δt (months)
1980-11-08	Eureka N41.08°W124.62°	7.2	0.444 (1980-08-01)	0.432 (1980-06-28)	0.445 (1980-08-01)	≈ 3
1989-10-18	Loma Prieta N37.04°W121.88°	7.0	-	-	-	-
1992-06-28	Landers N34.19°W116.46°	7.4	0.378 (1992-01-28)	0.377 (1992-01-03)	0.383 (1992-02-02)	≤ 5
<i>1994-01-17</i>	<i>Northridge</i> <i>N34.23°W118.55°</i>	<i>6.9</i>	<i>0.459</i> <i>(1993-11-14)</i>	<i>0.324</i> <i>(1993-10-18)</i>	<i>0.431</i> <i>(1993-11-14)</i>	≈ 2
1994-09-01	Mendocino N40.41°W126.30°	7.0	0.472 (1994-08-01)	0.474 (1994-07-11)	0.458 (1994-08-09)	≈ 1
1999-10-16	Hector Mine N34.60°W116.34°	7.0	0.444 (1999-05-14)	0.432 (1999-05-14)	0.422 (1999-05-15)	≈ 5
Fluctuation theorem and natural time analysis			0.46	0.45		

positive whereas when below negative. For this reason, we employ the relation

$$\frac{Pr(\beta_W - \beta_{W,0})}{Pr(\beta_{W,0} - \beta_W)} = \exp[\tau'(\beta_W - \beta_{W,0})], \quad (5)$$

which results from Eq.(1) when considering $A = \beta_W - \beta_{W,0}$ and experimentally determine $Pr(\beta_W - \beta_{W,0})$ by using bins of width $\Delta\beta_W = 0.01$. Figure 4 depicts the natural logarithm of the left hand side of Eq.(5) as a function of $(\beta_W - \beta_{W,0})$ for $W = 200$ and $W = 300$. In each case, the threshold $\beta_{W,0}$ is the one that maxi-

mizes the linear correlation coefficient (Pearson's r), thus pointing[53] to optimal linearity. We find the threshold values of $\beta_{200,0} = 0.45$ and $\beta_{300,0} = 0.46$. Moreover, the relative 'time-scale' τ' , which corresponds to the slope of Fig.4, lies in the range 40.6 to 48.3, which is comparable with a scale of the order of $l = 40$ sequential events used in the calculation of β_W .

Let us now compare the aforementioned threshold values $\beta_{200,0} = 0.45$ and $\beta_{300,0} = 0.46$ with the $\beta_{W,min}$ values identified before each mainshock in Table I. We find that except one mainshock, i.e., the Mendocino EQ in

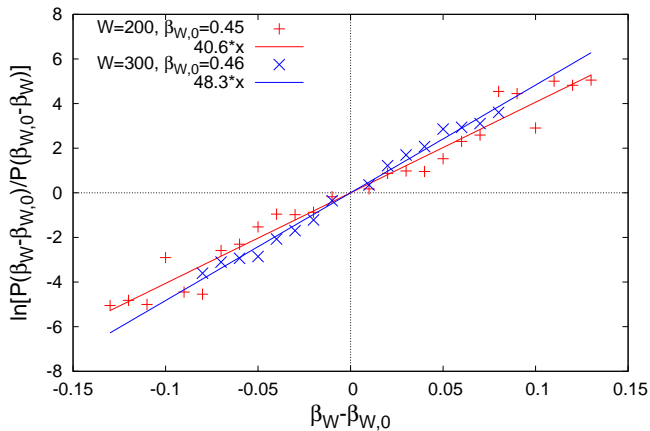


FIG. 4: Application of Eq.(5) for the experimentally determined β_W for $W = 200$ (red) and 300 (blue). The threshold values $\beta_{200,0} = 0.45$ and $\beta_{300,0} = 0.46$ are deduced from the maximization of the linear correlation coefficient (Pearson's) r , thus pointing[53] to optimal linearity.

1994, the other four mainshocks (including the strongest in Table I) led to $\beta_{200,min}$ and $\beta_{300,min}$ values that are lower than $\beta_{200,0}$ and $\beta_{300,0}$, respectively.

Thus, in summary, it may be considered that once the natural time analysis leads to an identification of precursory minima (i.e., $\beta_{200,min}$ and $\beta_{300,min}$) that are lower compared to the threshold $\beta_{W,0}$ values determined from the combined use of natural time analysis with the fluctuation theorem, a forthcoming major EQ is likely to occur.

Appendix: Interrelation of the variability β with correlations when a (natural) time window of fixed length is sliding through a time series

Here, we focus on the mean value $\mu \equiv \mathcal{E}(\kappa_1)$ of κ_1 and the corresponding standard deviation $\sigma \equiv$

$\sqrt{\mathcal{E}[\kappa_1 - \mathcal{E}(\kappa_1)]^2}$ when a (natural time) window of length l is sliding through a time series of $Q_k > 0, k = 1, 2, \dots, W$. Once these quantities have been evaluated, the variability β of κ_1 can then be estimated by $\beta \equiv \sigma/\mu$.

1. The mean value $\mu \equiv \mathcal{E}(\kappa_1)$ of κ_1

In a window of length l starting at $k = k_0$, the quantities

$$p_j(k_0) = \frac{Q_{k_0+j-1}}{\sum_{m=1}^l Q_{k_0+m-1}}, \quad j = 1, 2, \dots, l \quad (\text{A.1})$$

representing the normalized energy are obtained, which satisfy the necessary conditions

$$p_j(k_0) > 0, \quad (\text{A.2})$$

$$\sum_{j=1}^l p_j(k_0) = 1 \quad (\text{A.3})$$

to be considered as point probabilities. We can then define as usual[30, 55] the moments of the natural time $\chi_j = j/l$ as $\langle \chi^q \rangle = \sum_{j=1}^l (j/l)^q p_j(k_0)$ and hence

$$\kappa_1(k_0) = \sum_{j=1}^l \left(\frac{j}{l}\right)^2 p_j(k_0) - \left[\sum_{j=1}^l \frac{j}{l} p_j(k_0)\right]^2. \quad (\text{A.4})$$

Note that κ_1 is a non-linear functional of $\{p_j\}$.

Let us consider the average value μ_j of p_j obtained when the (natural time) window of length l slides through a time series of $Q_k > 0, k = 1, 2, \dots, W$, i.e., we have[56]

$$\mu_j \equiv \mathcal{E}(p_j) = \frac{1}{W-l+1} \sum_{k_0=1}^{W-l+1} p_j(k_0) = \frac{1}{W-l+1} \sum_{k_0=1}^{W-l+1} \frac{Q_{k_0+j-1}}{\sum_{m=1}^l Q_{k_0+m-1}}. \quad (\text{A.5})$$

It is obvious that the definition of Eq.(A.5) is consistent with Eq.(A.3), thus we have

$$\sum_{j=1}^l \mu_j = 1. \quad (\text{A.6})$$

Similarly for the second order moments of p_j , one can estimate[56] the variance of p_j by

$$\text{Var}(p_j) \equiv \mathcal{E}[(p_j - \mu_j)^2] = \frac{1}{W-l+1} \sum_{k_0=1}^{W-l+1} \left(\frac{Q_{k_0+j-1}}{\sum_{m=1}^l Q_{k_0+m-1}} - \mu_j \right)^2 \quad (\text{A.7})$$

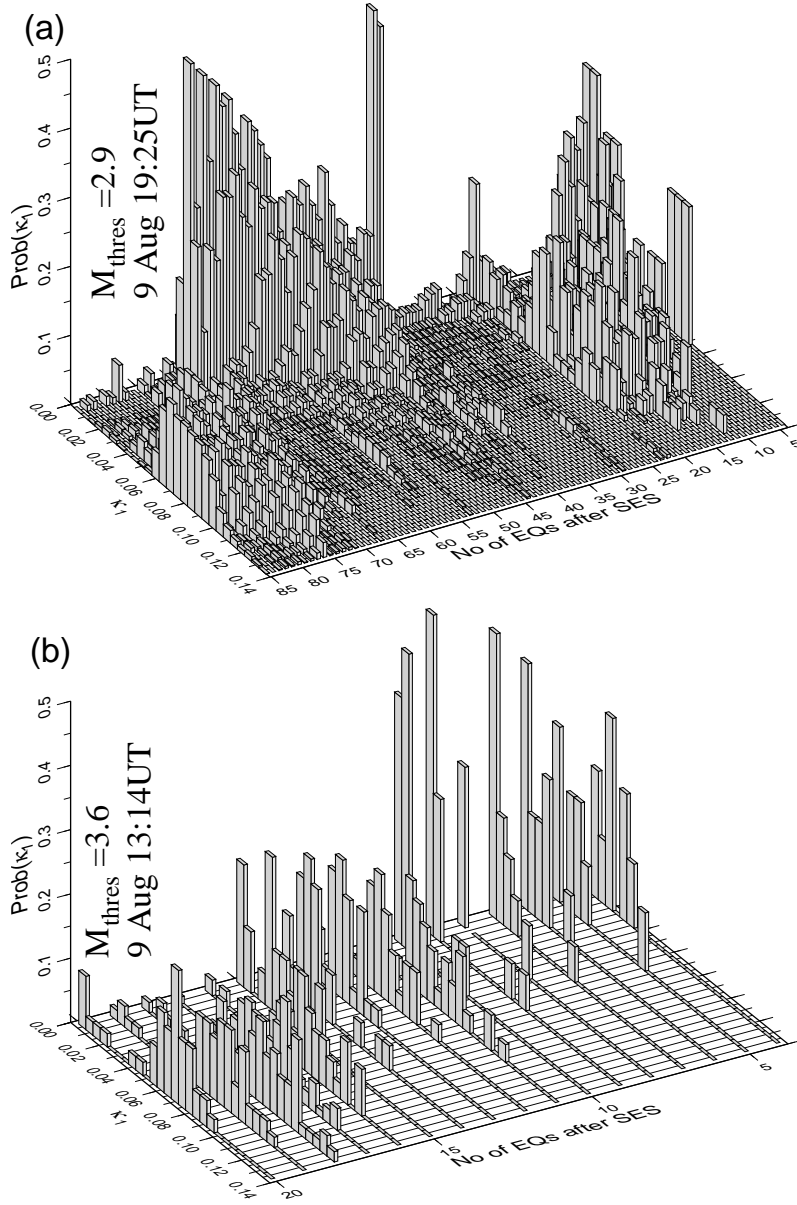


FIG. 5: The probability $\text{Prob}(\kappa_1)$ as it results from the analysis of seismicity that occurred after the initiation (at 02:30 UT on 31 March 2013) of the sequence of the additional SES activities from 31 March to 11 April 2013 (reported in the previous version of this manuscript on 13 June 2013) within the rectangular area depicted in the map (uppermost right) of Fig.2 for various magnitude thresholds M_{thres} . The date and time of the most recent earthquake considered into the calculation (upon the occurrence of which $\text{Prob}(\kappa_1)$ maximized at $\kappa_1 = 0.070$) is written in each case.

as well as the covariance

$$\begin{aligned} \text{Cov}(p_j, p_i) &\equiv \mathcal{E}[(p_j - \mu_j)(p_i - \mu_i)] \\ &= \frac{1}{W-l+1} \sum_{k_0=1}^{W-l+1} \left(\frac{Q_{k_0+j-1}}{\sum_{m=1}^l Q_{k_0+m-1}} - \mu_j \right) \left(\frac{Q_{k_0+i-1}}{\sum_{m=1}^l Q_{k_0+m-1}} - \mu_i \right). \end{aligned} \quad (\text{A.8})$$

In view of Eqs.(A.2) and(A.3), the quantities μ_j , $\text{Var}(p_j)$ and $\text{Cov}(p_j, p_m)$ are always finite irrespective of the existence of heavy tails in Q_k which is for example the case of seismicity. Moreover, for the purpose of our calculations the relation between the variance of p_j , $\text{Var}(p_j)$, and the covariance of p_j and p_m , $\text{Cov}(p_j, p_m)$, is important. Equations

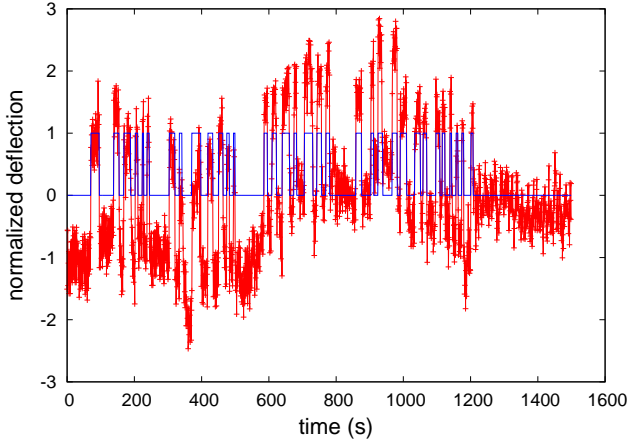


FIG. 6: The SES activity recorded on 8 February 2014 at the station VOL (near Volos city, central Greece). The normalized deflection versus time (lines with points) together with its dichotomous representation (lines without points). The data start at 17:05 UTC. The analysis of this SES activity in natural time resulted in the following values $\kappa_1 = 0.076(3)$, $S = 0.092(3)$, and $S_- = 0.076(3)$ which are compatible with those reported for SES activities (cf. S and S_- denote the entropy and the entropy under time reversal in natural time, see Chapter 3 and Table 4.6 of Ref.[32]).

(A.3) and (A.6) lead to

$$p_j - \mu_j = \sum_{m \neq j} (\mu_m - p_m), \quad (\text{A.9})$$

which when multiplied by $(p_j - \mu_j)$ and averaged (cf. $\hat{\mathcal{E}} \equiv \frac{1}{W-l+1} \sum_{k_0=1}^{W-l+1}$) results in

$$\text{Var}(p_j) = - \sum_{m \neq j} \text{Cov}(p_j, p_m). \quad (\text{A.10})$$

We now turn to the evaluation of the mean value μ of κ_1 obtained when the (natural time) window of length l slides through a time series of $Q_k > 0, k = 1, 2, \dots, W$,

$$\mu \equiv \mathcal{E}(\kappa_1) = \frac{1}{W-l+1} \sum_{k_0=1}^{W-l+1} \kappa_1(k_0), \quad (\text{A.11})$$

by studying its difference from the one that corresponds to the time series of the averages $\mathcal{M} = \{\mu_k\}$ which is labelled $\kappa_{1,\mathcal{M}}$,

$$\kappa_{1,\mathcal{M}} = \sum_{j=1}^l \left(\frac{j}{l}\right)^2 \mu_j - \left[\sum_{j=1}^l \frac{j}{l} \mu_j \right]^2. \quad (\text{A.12})$$

Hence,

$$\mu - \kappa_{1,\mathcal{M}} = \frac{1}{W-l+1} \sum_{k_0=1}^{W-l+1} \left\{ \sum_{m=1}^l \frac{m^2}{l^2} [p_m(k_0) - \mu_m] - \left[\sum_{m=1}^l \frac{m}{l} p_m(k_0) \right]^2 + \left(\sum_{m=1}^l \frac{m}{l} \mu_m \right)^2 \right\}. \quad (\text{A.13})$$

In view of the definition of μ_m , the first term in square brackets in the right hand side of Eq.(A.13) vanishes, whereas the latter two terms reduce to the opposite of the variance of

$$\langle \chi \rangle_{\mathcal{M}} = \sum_{m=1}^l \frac{m}{l} \mu_m, \quad (\text{A.14})$$

leading to

$$\mu - \kappa_{1,\mathcal{M}} = -\frac{1}{W-l+1} \sum_{k_0=1}^{W-l+1} \left\{ \sum_{m=1}^l \frac{m}{l} [p_m(k_0) - \mu_m] \right\}^2. \quad (\text{A.15})$$

Expanding the term within the curly brackets and interchanging the summations, we get

$$\kappa_{1,\mathcal{M}} - \mu = \sum_{m=1}^l \frac{m^2}{l^2} \text{Var}(p_m) + 2 \sum_{j=1}^{l-1} \sum_{m=j+1}^l \frac{jm}{l^2} \text{Cov}(p_j, p_m). \quad (\text{A.16})$$

which, upon using Eq.(A.10), leads to

$$\mu - \kappa_{1,\mathcal{M}} = \sum_{j=1}^{l-1} \sum_{m=j+1}^l \frac{(j-m)^2}{l^2} \text{Cov}(p_j, p_m) = \frac{1}{2} \sum_{j=1}^l \sum_{m=1}^l \frac{(j-m)^2}{l^2} \text{Cov}(p_j, p_m). \quad (\text{A.17})$$

The latter relation turns to

$$\mu = \kappa_{1,\mathcal{M}} + \sum_{\text{all pairs}} \frac{(j-m)^2}{l^2} \text{Cov}(p_j, p_m) \quad (\text{A.18})$$

where $\sum_{\text{all pairs}} \equiv \sum_{j=1}^{l-1} \sum_{m=j+1}^l$.

Equation (A.18) shows that the mean value μ itself is a measure of the correlations between successive earthquake magnitudes. The practical use of this equation, however, in order to estimate the strength of these correlations between seismic events requires[32, 56–59] the construction of a large number of shuffled copies of the original earthquake catalog and a comparison of μ with the relevant distribution obtained from the shuffled copies. Obviously, this task becomes cumbersome when the (natural time) window of length l is sliding through a long time series of Q_k .

When Q_k are independent and identically distributed positive random variables, Eq.(A.18) results[32, 57] in

$$\mu = \kappa_u \left(1 - \frac{1}{l^2} \right) - \kappa_u(l+1) \text{Var}(p), \quad (\text{A.19})$$

where $\kappa_u = 1/12$ -corresponding to the κ_1 value for the uniform distribution- and $\text{Var}(p)$ the variance of any p_j .

2. The standard deviation σ of the κ_1 values

Let us now investigate the standard deviation σ of the κ_1 values obtained when the (natural time) window of length l slides through a time series of Q_k . This is obtained from the variance

$$\sigma^2 = \text{Var}(\kappa_1) \equiv \mathcal{E}[(\kappa_1 - \mu)^2] = \frac{1}{W-l+1} \sum_{k_0=1}^{W-l+1} [\kappa_1(k_0) - \mu]^2. \quad (\text{A.20})$$

Numerically, the above quantity can be evaluated almost as easily as μ when $\kappa_1(k_0)$ are available.

In order to obtain an analytical expression, by inserting Eq.(A.18) into (A.20), we obtain

$$\begin{aligned} \sigma^2 &= \frac{1}{W-l+1} \sum_{k_0=1}^{W-l+1} \left\{ \sum_{m=1}^l \frac{m^2}{l^2} [p_m(k_0) - \mu_m] - \left[\sum_{m=1}^l \frac{m}{l} p_m(k_0) \right]^2 \right. \\ &\quad \left. + \left(\sum_{m=1}^l \frac{m}{l} \mu_m \right)^2 - \sum_{\text{all pairs}} \frac{(j-m)^2}{l^2} \text{Cov}(p_j, p_m) \right\}^2. \end{aligned} \quad (\text{A.21})$$

Rearranging the terms

$$\begin{aligned} \left[\sum_{m=1}^l \frac{m}{l} p_m(k_0) \right]^2 - \left(\sum_{m=1}^l \frac{m}{l} \mu_m \right)^2 &= \left\{ \sum_{m=1}^l \frac{m}{l} [p_m(k_0) - \mu_m] \right\} \left\{ \sum_{m=1}^l \frac{m}{l} [p_m(k_0) + \mu_m] \right\} \\ &= \left\{ \sum_{m=1}^l \frac{m}{l} [p_m(k_0) - \mu_m] \right\}^2 + 2 \langle \chi \rangle_{\mathcal{M}} \left\{ \sum_{m=1}^l \frac{m}{l} [p_m(k_0) - \mu_m] \right\} \end{aligned} \quad (\text{A.22})$$

we get

$$\begin{aligned} \sigma^2 = & \frac{1}{W-l+1} \sum_{k_0=1}^{W-l+1} \left[\sum_{m=1}^l \left(\frac{m^2}{l^2} - 2\langle \chi \rangle_{\mathcal{M}} \frac{m}{l} \right) [p_m(k_0) - \mu_m] - \left\{ \sum_{m=1}^l \frac{m}{l} [p_m(k_0) - \mu_m] \right\}^2 \right. \\ & \left. - \sum_{\text{all pairs}} \frac{(j-m)^2}{l^2} \text{Cov}(p_j, p_m) \right]^2. \end{aligned} \quad (\text{A.23})$$

Upon expanding the square over the square brackets in Eq.(A.23) we obtain six terms:

$$\sigma^2 = \frac{1}{W-l+1} \sum_{k_0=1}^{W-l+1} \left\{ \sum_{m=1}^l \left(\frac{m^2}{l^2} - 2\langle \chi \rangle_{\mathcal{M}} \frac{m}{l} \right) [p_m(k_0) - \mu_m] \right\}^2 \quad (\text{A.24a})$$

$$- \frac{2}{W-l+1} \sum_{k_0=1}^{W-l+1} \left\{ \sum_{m=1}^l \left(\frac{m^2}{l^2} - 2\langle \chi \rangle_{\mathcal{M}} \frac{m}{l} \right) [p_m(k_0) - \mu_m] \right\} \left\{ \sum_{m=1}^l \frac{m}{l} [p_m(k_0) - \mu_m] \right\}^2 \quad (\text{A.24b})$$

$$- \left[\sum_{\text{all pairs}} \frac{(j-m)^2}{l^2} \text{Cov}(p_j, p_m) \right] \frac{2}{W-l+1} \sum_{k_0=1}^{W-l+1} \left\{ \sum_{m=1}^l \left(\frac{m^2}{l^2} - 2\langle \chi \rangle_{\mathcal{M}} \frac{m}{l} \right) [p_m(k_0) - \mu_m] \right\} \quad (\text{A.24c})$$

$$+ \frac{1}{W-l+1} \sum_{k_0=1}^{W-l+1} \left\{ \sum_{m=1}^l \frac{m}{l} [p_m(k_0) - \mu_m] \right\}^4 \quad (\text{A.24d})$$

$$+ \left[\sum_{\text{all pairs}} \frac{(j-m)^2}{l^2} \text{Cov}(p_j, p_m) \right] \frac{2}{W-l+1} \sum_{k_0=1}^{W-l+1} \left\{ \sum_{m=1}^l \frac{m}{l} [p_m(k_0) - \mu_m] \right\}^2 \quad (\text{A.24e})$$

$$+ \left[\sum_{\text{all pairs}} \frac{(j-m)^2}{l^2} \text{Cov}(p_j, p_m) \right]^2. \quad (\text{A.24f})$$

The following comments are in order: First, the term in (A.24c) vanishes due to Eq.(A.5). Second, the terms in (A.24b) and (A.24d) clearly depend on moment correlations higher than the second, thus they should be neglected when restricting ourselves to second order correlations. Third, the second term in (A.24e) can be evaluated using Eqs.(A.15) and (A.17) leading to a partial cancellation with the term in (A.24f). Hence, *restricting ourselves to second order correlations*, we finally obtain

$$\sigma^2 = \frac{1}{W-l+1} \sum_{k_0=1}^{W-l+1} \left\{ \sum_{m=1}^l \left(\frac{m^2}{l^2} - 2\langle \chi \rangle_{\mathcal{M}} \frac{m}{l} \right) [p_m(k_0) - \mu_m] \right\}^2 - \left[\sum_{\text{all pairs}} \frac{(j-m)^2}{l^2} \text{Cov}(p_j, p_m) \right]^2. \quad (\text{A.25})$$

The first term in Eq.(A.25) can be evaluated by expanding the square over the curly brackets and using Eq.(A.10) -in a way similar to Eqs.(A.16) and (A.17)- so that we obtain

$$\sigma^2 = - \sum_{\text{all pairs}} \left[\left(\frac{m}{l} - \langle \chi \rangle_{\mathcal{M}} \right)^2 - \left(\frac{j}{l} - \langle \chi \rangle_{\mathcal{M}} \right)^2 \right]^2 \text{Cov}(p_j, p_m) - \left[\sum_{\text{all pairs}} \frac{(j-m)^2}{l^2} \text{Cov}(p_j, p_m) \right]^2. \quad (\text{A.26})$$

Equation (A.26) reveals that σ^2 -like the mean value μ in Eq.(A.18)- is a measure of the correlations, but σ^2 is almost proportional (see also below) to these correlations whereas in μ they appear as an additive term in Eq.(A.18).

3. The variability σ/μ

By combining Eqs.(A.18) and (A.26) we find:

$$\beta = \frac{\sqrt{-\sum_{\text{all pairs}} \left[\left(\frac{m}{l} - \langle \chi \rangle_{\mathcal{M}} \right)^2 - \left(\frac{j}{l} - \langle \chi \rangle_{\mathcal{M}} \right)^2 \right]^2 \text{Cov}(p_j, p_m) - \left[\sum_{\text{all pairs}} \frac{(j-m)^2}{l^2} \text{Cov}(p_j, p_m) \right]^2}}{\kappa_{1,\mathcal{M}} + \sum_{\text{all pairs}} \frac{(j-m)^2}{l^2} \text{Cov}(p_j, p_m)}. \quad (\text{A.27})$$

This equation, which is just Eq.(4) of the main text, provides in general the interrelation between the variability β and the event correlations.

Additional insight on the physical meaning of σ/μ may be obtained when adopting the paradigm of the uniform distribution[32, 36, 37] which corresponds to a simple system operating at stationarity, i.e., when Q_k are independent and identically distributed positive random variables. In this case, we have[32]

$$\mu_j = \frac{1}{l}, \quad (\text{A.28})$$

$$\langle \chi \rangle_{\mathcal{M}} = \sum_{m=1}^l \frac{m}{l^2} = \frac{1}{2} + \frac{1}{2l}, \quad (\text{A.29})$$

and due to Eq.(A.10)

$$\text{Cov}(p_j, p_m) = -\frac{\text{Var}(p)}{(l-1)}, \quad (\text{A.30})$$

thus we obtain

$$\sigma^2 = \frac{\text{Var}(p)}{(l-1)} \left\{ \sum_{\text{all pairs}} \left[\left(\frac{m}{l} - \frac{1}{2} - \frac{1}{2l} \right)^2 - \left(\frac{j}{l} - \frac{1}{2} - \frac{1}{2l} \right)^2 \right]^2 - \frac{\text{Var}(p)}{(l-1)} \left[\sum_{\text{all pairs}} \frac{(j-m)^2}{l^2} \right]^2 \right\}. \quad (\text{A.31})$$

For large l the summations over all pairs can be effectively, e.g. $l > 10$, approximated by integrations

$$\sum_{\text{all pairs}} \left[\left(\frac{m}{l} - \frac{1}{2} - \frac{1}{2l} \right)^2 - \left(\frac{j}{l} - \frac{1}{2} - \frac{1}{2l} \right)^2 \right]^2 \approx \frac{l^2}{2} \int_0^1 \int_0^1 \left[\left(\chi - \frac{1}{2} \right)^2 - \left(\psi - \frac{1}{2} \right)^2 \right]^2 d\chi d\psi = \frac{l^2}{180}, \quad (\text{A.32})$$

$$\sum_{\text{all pairs}} \frac{(j-m)^2}{l^2} \approx \frac{l^2}{2} \int_0^1 \int_0^1 (\chi - \psi)^2 d\chi d\psi = \frac{l^2}{12} \quad (\text{A.33})$$

Equation (A.31) simplifies to

$$\sigma^2 \approx l \text{Var}(p) \kappa_u^2 \left[\frac{4}{5} - l \text{Var}(p) \right], \quad (\text{A.34})$$

and Eq.(A.19) becomes

$$\mu \approx \kappa_u [1 - l \text{Var}(p)]. \quad (\text{A.35})$$

Thus, the variability simply results in

$$\beta = \frac{\sigma}{\mu} = \sqrt{l \text{Var}(p)} \left[\frac{\sqrt{\frac{4}{5} - l \text{Var}(p)}}{1 - l \text{Var}(p)} \right]. \quad (\text{A.36})$$

When Q_k exhibit heavy tails as in the case for seismicity, the quantity $l \text{Var}(p)$ measures the intensity of such tails and so does β . In other words, for randomly shuffled earthquake data or earthquakes occurring with temporally uncorrelated magnitudes, the variability β is a measure of the b -value of the Gutenberg-Richter law. Since real seismic data may also exhibit temporal correlations between earthquake magnitudes[27, 32, 56–60], the

general expression of the variability obtained above (i.e., Eq.(A.27)) from Eqs.(A.18) and (A.26) captures both the effects of correlations and heavy-tails.

When Q_k do not exhibit heavy tails, which is not of course the case of seismicity, the quantity $l \text{Var}(p)$ is simply related[32, 61] to the mean μ_0 and the standard deviation σ_0 of Q_k :

$$l \text{Var}(p) = \frac{1}{l} \frac{\sigma_0^2}{\mu_0^2}. \quad (\text{A.37})$$

Assuming that σ_0/μ_0 is of the order of unity, $l \text{Var}(p)$ becomes small compared to unity when $l > 10$, and Eq.(A.36) becomes

$$\beta = \frac{\sigma}{\mu} = \frac{2}{\sqrt{5}} \frac{\sigma_0}{\mu_0} \left(\frac{1}{\sqrt{l}} \right), \quad (\text{A.38})$$

i.e., the variability of κ_1 is directly proportional to the variability of the data Q_k . Note that the same holds for the standard deviation of the natural time entropy[32, 61] S as well as for change ΔS of the entropy in natural time under time reversal[32, 62] (cf. for the analysis in

natural time under time reversal, see also Refs.[63] and [64]). Thus, in this case, one could alternatively view β

as an entropic measure.

-
- [1] I. J. Ford and R. E. Spinney, Phys. Rev. E **86**, 021127 (2012).
- [2] C. Gardiner, *Stochastic Methods: A Handbook for the Natural and Social Sciences* (Springer, New York, 2009).
- [3] U. Seifert, Phys. Rev. Lett. **95**, 040602 (2005).
- [4] U. Seifert, Eur. Phys. J. B **64**, 423 (2008).
- [5] K. Sekimoto, *Stochastic Energetics, Lecture Notes in Physics No.799* (Springer, Berlin, Heidelberg, 2010).
- [6] D. J. Evans, S. R. Williams, and D. J. Searles, J. Chem. Phys. **135**, 194107 (2011).
- [7] D. J. Evans, E. G. D. Cohen, and G. P. Morriss, Phys. Rev. Lett. **71**, 2401 (1993).
- [8] U. M. B. Marconi, A. Puglisi, L. Rondoni, and A. Vulpiani, Physics Reports **461**, 111 (2008).
- [9] D. J. Evans and D. J. Searles, Phys. Rev. E **50**, 1645 (1994).
- [10] D. J. Evans and D. J. Searles, Adv. Phys **51**, 1529 (2002).
- [11] D. J. Searles and D. J. Evans, Aust. J. Chem. **57**, 1119 (2004).
- [12] D. J. Evans, S. R. Williams, and D. J. Searles, J. Chem. Phys. **134**, 204113 (2011).
- [13] D. J. Searles and D. J. Evans, J. Chem. Phys. **113**, 3503 (2000).
- [14] J. C. Reid, D. J. Evans, and D. J. Searles, J. Chem. Phys. **136**, 021101 (2012).
- [15] D. J. Evans and D. J. Searles, Phys. Rev. E **52**, 5839 (1995).
- [16] D. J. Evans and D. J. Searles, Phys. Rev. E **53**, 5808 (1996).
- [17] D. J. Searles, G. Ayton, and D. J. Evans, AIP Conf. Proc. **519**, 271 (2000).
- [18] G. Gallavotti and E. G. D. Cohen, Phys. Rev. Lett. **74**, 2694 (1995).
- [19] G. Gallavotti and E. G. D. Cohen, J. Stat. Phys. **80**, 931 (1995).
- [20] D. J. Evans, D. J. Searles, and E. Mittag, Phys. Rev. E **63**, 051105 (2001).
- [21] J. L. Lobowitz and H. Spohn, J. Stat. Phys. **95**, 333 (1999).
- [22] D. J. Searles and D. J. Evans, Phys. Rev. E **60**, 159 (1999).
- [23] D. L. Turcotte, *Fractals and Chaos in Geology and Geophysics* (Cambridge University Press, Cambridge, 1997), 2nd ed.
- [24] J. R. Holliday, J. B. Rundle, D. L. Turcotte, W. Klein, K. F. Tiampo, and A. Donnellan, Phys. Rev. Lett. **97**, 238501 (2006).
- [25] J. N. Tenenbaum, S. Havlin, and H. E. Stanley, Phys. Rev. E **86**, 046107 (2012).
- [26] S. Lennartz, A. Bunde, and D. L. Turcotte, Geophys. J. Int. **184**, 1214 (2011).
- [27] E. Lippiello, C. Godano, and L. de Arcangelis, Geophys. Res. Lett. **39**, L05309 (2012).
- [28] L. Telesca, Tectonophysics **494**, 155 (2010).
- [29] Q. Huang, Geophys. Res. Lett. **35**, L23308 (2008).
- [30] P. A. Varotsos, N. V. Sarlis, and E. S. Skordas, Phys. Rev. E **66**, 011902 (2002).
- [31] P. Varotsos, N. V. Sarlis, E. S. Skordas, S. Uyeda, and M. Kamogawa, Proc. Natl. Acad. Sci. USA **108**, 11361 (2011).
- [32] P. A. Varotsos, N. V. Sarlis, and E. S. Skordas, *Natural Time Analysis: The new view of time. Precursory Seismic Electric Signals, Earthquakes and other Complex Time-Series* (Springer-Verlag, Berlin Heidelberg, 2011).
- [33] P. A. Varotsos, N. V. Sarlis, H. K. Tanaka, and E. S. Skordas, Phys. Rev. E **72**, 041103 (2005).
- [34] P. Varotsos, N. Sarlis, and E. Skordas, EPL **99**, 59001 (2012).
- [35] H. Kanamori, Nature **271**, 411 (1978).
- [36] P. A. Varotsos, N. V. Sarlis, and E. S. Skordas, Phys. Rev. E **68**, 031106 (2003).
- [37] P. A. Varotsos, N. V. Sarlis, and E. S. Skordas, Phys. Rev. E **67**, 021109 (2003).
- [38] N. V. Sarlis, E. S. Skordas, and P. A. Varotsos, EPL **91**, 59001 (2010).
- [39] P. Varotsos and K. Alexopoulos, Tectonophysics **110**, 73 (1984).
- [40] P. Varotsos and K. Alexopoulos, Tectonophysics **110**, 99 (1984).
- [41] P. Varotsos and K. Alexopoulos, *Thermodynamics of Point Defects and their Relation with Bulk Properties* (North Holland, Amsterdam, 1986).
- [42] P. Varotsos, K. Alexopoulos, and M. Lazaridou, Tectonophysics **224**, 1 (1993).
- [43] P. Varotsos and M. Lazaridou, Tectonophysics **188**, 321 (1991).
- [44] P. Varotsos, *The Physics of Seismic Electric Signals* (TERRAPUB, Tokyo, 2005).
- [45] N. V. Sarlis, E. S. Skordas, M. S. Lazaridou, and P. A. Varotsos, Proc. Japan Acad., Ser. B **84**, 331 (2008).
- [46] *Note added on 13 August 2013.* At 09:06 UT on 7 August 2013 an M_w 5.3 EQ occurred with an epicenter at 38.70°N 22.68°E lying inside the area $N_{37.7}^{39.0} E_{22.6}^{24.2}$ (depicted in the uppermost right part of Fig.2) estimated in the previous version of this manuscript on 13 June 2013. Here, we present the results of the analysis of seismicity that occurred after the initiation (at 02:30 UT on 31 March 2013) of the sequence of the additional SES activities at LAM from 31 March to 11 April 2013 (this is the longest duration we ever observed in Greece). Applying the procedure developed in Ref.[45], the following results were obtained clarifying that our study was intentionally extended after the occurrence of the aforementioned M_w 5.3 EQ until at 02:51 UT on 12 August 2013: The probability $\text{Prob}(\kappa_1)$ of the κ_1 values of seismicity in the *same* area, i.e., $N_{37.7}^{39.0} E_{22.6}^{24.2}$, maximized at $\kappa_1 = 0.070$ at times between 13:10 UT and 19:49 UT on 9 August 2013 exhibiting magnitude threshold invariance in the broad magnitude range $M_{thres} = 2.6$ to 3.6 (which suggests that the system approaches the critical point), for example see Fig.5. In addition, the analysis in the magnitude range comprising lower thresholds, i.e., $M_{thres} = 2.4$ to 2.6 (for which however the completeness of the seismic catalog is unclear, as mentioned), showed that $\text{Prob}(\kappa_1)$

also maximized at $\kappa_1 = 0.070$ upon the occurrence of small events a few minutes before the $M_w 5.3$ EQ.

- [47] *Note added on 15 October 2013.* Actually, a $M_w 5.3$ EQ occurred on 16 September 2013 with an epicenter at $38.71^\circ\text{N } 22.73^\circ\text{E}$, i.e., inside the rectangular area depicted in Fig. 2 (uppermost right). Hence, the two EQs, i.e., the one on 7 August and the $M_w 5.3$ on 16 September 2013, were preceded by the aforementioned SES activities (recorded during 31 March - 11 April 2013) and occurred after the κ_1 value in the candidate area approached the value $\kappa_1=0.070$ (cf. the exact dates of this approach have to be reconsidered, which will be discussed in detail elsewhere; recall that, as mentioned, the completeness of the seismic catalogue used at that time for the low magnitude thresholds, could not be checked with confidence). In the meantime, new SES activities were recorded at LAM on 1, 4 and 11-14 October 2013 with polarity different from that of the earlier ones. This difference is strikingly reminiscent of the case discussed in p.344 (left column) of Ref. [43]. Thus, we currently investigate as in Ref. [45] the seismicity after 1 October 2013 within the same area $N_{37.7}^{39.0} E_{22.6}^{24.2}$ in order to identify when the system may approach the critical point.
- [48] *Note added on 15 December 2013.* The investigation mentioned in the previous Note concerning the evolution of seismicity within the area $N_{37.7}^{39.0} E_{22.6}^{24.2}$ (uppermost right in Fig.2) after 1 October 2013 (i.e., after the initiation of the aforementioned three SES activities at LAM on 1, 4 and 11-14 October 2013), led to the following result: The probability $\text{Prob}(\kappa_1)$ maximized at $\kappa_1 = 0.070$ on 9 November 2013, which was followed by an $M_L = 4.9$ EQ -i.e., $M_s(ATH) = M_L + 0.5 = 5.4-$ on 12 November 2013 with an epicenter at $38.9^\circ\text{N } 23.1^\circ\text{E}$ as well as by two $M_L = 4.2$ EQs that occurred later, i.e., on 22 November and 11 December 2013 with epicenters at $39.05^\circ\text{N } 22.41^\circ\text{E}$ and $39.01^\circ\text{N } 22.29^\circ\text{E}$, respectively. In other words, these three EQs occurred at epicenters lying a few tens of km to the East (the first EQ) as well as to the West (the latter two) of the epicenters of the previous EQs on 7 August 2013 and 16 September 2013. Such a displacement of the epicenters is consistent with the change of the SES polarity [43] commented in the previous Note dated on 15 October 2013. It is challenging that additional SES activities were recorded at LAM on 6 & 7, 14 & 15 and 22 & 23 November 2013 as well as on 6-13 December 2013, which instigated a new investigation of the subsequent seismicity inside the area $N_{37.7}^{39.0} E_{22.6}^{24.2}$ (and its possible extension to the West by $\approx 0.3^\circ$) to identify when the system may again approach to the critical point.
- [49] *Note added on 26 February 2014.* In continuation of the previous Note, we mention that on 8 February 2014 an SES activity was recorded at VOL (see Fig.6). This implies that a supplemental study of the subsequent seismicity in natural time should be carried out in the rectangular area depicted in Fig.2 extended by $\approx 0.3^\circ$ to the North (surrounding also the VOL measuring station) in order to determine when the system may approach the critical point.
- [50] *Note added on 7 August 2014.* An SES activity of dichotomous nature as in the lower three channels of Fig.1(b) was recorded on 27 July 2014 at KER. Thus, a new analysis in natural time of the subsequent seismicity within the rectangular area depicted in the uppermost right part of Fig.2 is carried out in order to identify when the system may approach the critical point.
- [51] *Note added on 16 January 2015.* Actually on 17 November 2014 two EQs of $M_s(ATH) = 5.7$ occurred with an epicenter at $38.64^\circ\text{N } 23.40^\circ\text{E}$, i.e., very close to the center of the expected area shown in the uppermost right part of Fig.2. A new SES activity was recorded again at KER on 24 December 2014. It has been empirically observed (see p. 15 of Ref.[32]) that the strongest EQ usually occurs during the fourth week after the initiation of the SES activity; otherwise, smaller EQs appear during this week and the strongest EQ occurs after an additional period of 2-3 weeks. To identify the occurrence time of the strongest EQ with better accuracy (i.e., a few days or so), however, we compute for the expected area the κ_1 value of the seismicity subsequent to the SES activity and determine when it converges to the critical value $\kappa_1 = 0.070$. This is currently carried out for the present case by considering the seismicity within the rectangular area depicted in the uppermost right part of Fig.2 (which includes of course the $M_s(ATH) = 3.7$ EQ that occurred today at 06:32 UT with epicenter $38.03^\circ\text{N } 23.76^\circ\text{E}$).
- [52] P. A. Varotsos, N. V. Sarlis, E. S. Skordas, and M. S. Lazaridou, *Tectonophysics* **589**, 116 (2013).
- [53] W. H. Press, S. Teukolsky, W. Vetterling, and B. P. Flannery, *Numerical Recipes in FORTRAN* (Cambridge University Press, New York, 1992).
- [54] C.-K. Peng, S. V. Buldyrev, S. Havlin, M. Simons, H. E. Stanley, and A. L. Goldberger, *Phys. Rev. E* **49**, 1685 (1994).
- [55] P. A. Varotsos, N. V. Sarlis, and E. S. Skordas, *Practica of Athens Academy* **76**, 294 (2001).
- [56] N. V. Sarlis and S.-R. G. Christopoulos, *CHAOS* **22**, 023123 (2012).
- [57] P. A. Varotsos, N. V. Sarlis, E. S. Skordas, H. K. Tanaka, and M. S. Lazaridou, *Phys. Rev. E* **74**, 021123 (2006).
- [58] N. V. Sarlis, E. S. Skordas, and P. A. Varotsos, *Phys. Rev. E* **80**, 022102 (2009).
- [59] N. V. Sarlis, *Phys. Rev. E* **84**, 022101 (2011).
- [60] E. Lippiello, C. Godano, and L. de Arcangelis, *Phys. Rev. Lett.* **98**, 098501 (2007).
- [61] P. A. Varotsos, N. V. Sarlis, E. S. Skordas, and M. S. Lazaridou, *Phys. Rev. E* **70**, 011106 (2004).
- [62] P. A. Varotsos, N. V. Sarlis, E. S. Skordas, and M. S. Lazaridou, *Appl. Phys. Lett.* **91**, 064106 (2007).
- [63] P. A. Varotsos, N. V. Sarlis, E. S. Skordas, H. K. Tanaka, and M. S. Lazaridou, *Phys. Rev. E* **73**, 031114 (2006).
- [64] P. A. Varotsos, N. V. Sarlis, E. S. Skordas, and M. S. Lazaridou, *J. Appl. Phys.* **103**, 014906 (2008).